Original article

Nuclear Medicine Communications

Comparative values of gated blood-pool SPECT and CMR for ejection fraction and volume estimation

Louis Sibille[a], Fayçal Ben Bouallegue[a], Aurélie Bourdon[a], Antoine Micheau[b], Hélène Vernhet-Kovacsik[b] and Denis Mariano-Goulart[a]

Objective **Gated blood-pool single-photon emission computed tomography (GBPS) was compared with cardiac magnetic resonance (CMR) for the measurement of left ventricular (LV) and right ventricular (RV) ejection fractions (EF) and volumes [end-diastolic volume (EDV) or end-systolic volume (ESV)] in a mixed population.**

Methods **Thirty patients (70% men; mean age: 61 ± 14 years) referred for various symptoms or heart diseases, predominantly ischemic, were included. GBPS data were analyzed using segmentation software described earlier based on the watershed algorithm. CMR images were acquired for both ventricles at the same time using a steady-state-free precession sequence and short-axis views. No compensation for papillary muscles was used. LVEF and RVEF and volumes were assessed with GBPS and CMR and were compared.**

Results **LVEF and volumes were correlated ($P<0.001$). The difference in LVEF between GBPS and CMR was not significant ($P=0.063$). The limits of agreement were close for LVEF (−11 to 15%) and wider for LV volumes (−82 to 11 ml for EDV and −52 to 15 ml for ESV), with higher volume values obtained with CMR (mean differences of 36 ± 24 ml for EDV and 19 ± 17 ml for ESV). The RVEF and volumes assessed by GBPS and CMR were correlated ($P<0.001$). The difference in RVESV between GBPS or CMR was not significant ($P=0.136$). The limits of agreement were relatively close for all RV parameters (−15 to 8% for EF; −44 to 22 ml for EDV, and −25 to 21 ml for ESV). In 24 patients without valvulopathy or shunt, the difference between LV stroke volume and RV stroke volume was lower with GBPS than with CMR (9 ± 14 ml and 18 ± 13 ml, respectively, with $P=0.027$).**

Conclusion **GBPS is a simple and widely available technique that can assess both LVEF and RVEF, and volumes with slight differences compared with CMR.** *Nucl Med Commun* **32:121–128 © 2011 Wolters Kluwer Health | Lippincott Williams & Wilkins.**

Nuclear Medicine Communications 2011, **32**:121–128

Keywords: ejection fraction, gated blood-pool imaging, magnetic resonance imaging, single-photon emission computed tomography, ventricular volume

[a]Department of Nuclear Medicine, CHRU Lapeyronie and [b]Department of Thoracic and Cardiovascular Imaging, CHRU Arnaud de Villeneuve, Montpellier, France

Correspondence to Dr Louis Sibille, MD, Department of Nuclear Medicine, CHRU Lapeyronie 371, Avenue du Doyen Gaston Giraud, 34295 Montpellier, France
Tel: +33 467339517; fax: +33 467338465;
e-mail: louis.sibille@gmail.com

Received 9 September 2010 **Revised** 7 October 2010
Accepted 8 October 2010

Introduction

Accurate quantification of ventricular function and volumes is important in the management of patients with cardiovascular disease. In patients with coronary artery disease, left ventricular (LV) ejection fraction (EF) at rest or stress, end-diastolic volume (EDV), and end-systolic volume (ESV) are strong independent predictors of cardiovascular morbidity and death [1,2]. Even patients without earlier myocardial infarction or valvular disease are at high risk of congestive heart failure and death when only a mild impairment of LVEF is present [3]. Right ventricular (RV) EF is also a very important parameter, which, independently of pulmonary hypertension, improves the accuracy of the prognostic stratification of patients with heart failure [4].

Several imaging techniques can be used to assess EF and ventricular volumes. Availability, innocuousness, and cost made echocardiography the most frequently used technique in spite of high interobserver variability and the requirement of a geometrical assumption to define LV and RV volumes. Several factors may affect the measurement of LV function in gated single-photon emission computed tomography perfusion imaging, such as areas of marked hypoperfusion [5–8]. The limitations of planar gated blood pool are overlapping structures and difficult assessment of RV function using the first-pass technique [9].

Thanks to the combination of excellent spatial, contrast, and temporal resolution, that cardiac magnetic resonance (CMR) imaging has become a useful tool for assessing cardiac performance in an accurate and reproducible way [10–13]. A new steady-state-free precession sequence has improved the contrast between the myocardium and the cavity, allowing significantly better detection of the endocardial border [14]. Simpson's rule as a geometrical model is far more accurate than that used in contrast

0143-3636 DOI: 10.1097/MNM.0b013e32834155f1

ventriculography, echocardiography (M-mode and two-dimensional), or myocardial perfusion scintigraphy [15,16]. This approach is usually more time-consuming for both image acquisition and postprocessing, and it also requires highly qualified staff. Similarly, CMR is not widely available and is of limited feasibility for patients with implanted devices or claustrophobia.

Gated blood-pool single-photon emission computed tomography (GBPS) is a technically simple and widely available count-based method that is independent of geometry. Thus, it may permit simultaneous assessment at equilibrium of the LV and RV parameters [9,17,18]. Regional ventricular function measurements such as local EF or local times of end-systole are also available with this technique [19–22].

In this study, we investigated the correlation and agreement between LVEF and RVEF and volume measurements derived from GBPS data and those obtained with the CMR method as the correlative standard.

Materials and methods

Patients

Thirty consecutive patients [aged 61 ± 14 years (range: 34–87 years); 70% men] were prospectively included in this study. All patients had clinical indications for CMR studies and isotopic evaluation of EF to diagnose cardiac disease or as follow-up. The reasons for referral were coronaropathy ($n = 16$), myocarditis ($n = 4$), arrhythmogenic RV dysplasia ($n = 2$), constrictive pericarditis ($n = 2$), pulmonary hypertension ($n = 4$), cardiac involvement in scleroderma ($n = 1$), and adrenergic cardiomyopathy ($n = 1$). All patients were prospectively recruited from inpatient and outpatient populations at the Montpellier University Hospital between 2 August 2008 and 15 June 2009.

All correlative GBPS and CMR studies were carried out within a mean interval of 12 ± 21 days (median: 2 days; range: 0–81 days). No patient had any significant cardiac event between the studies, and none had changes in medical or surgical therapy. All patients gave their informed consent before inclusion in the study.

Cardiac magnetic resonance data acquisition

CMR data were collected on a 1.5-T scanner (Magnetom Sonata; Siemens Medical Solutions, Erlangen, Germany). Breath-hold TrueFISP (Siemens Medical Solutions) cine CMR was used [23]. The integrated parallel acquisition technique was required in six cases.

Multiplane localizers identified the cardiac position and the usual cardiac imaging planes using a standard iterative scouting technique. Retrospective ECG-gated cine CMR images were then acquired using a segmented steady-state precession sequence, TrueFISP. Ten to 12 short-axis views that encompassed the entire LV and RV were acquired using the following parameters from the Society for Cardiovascular Magnetic Resonance [24]: slice thickness 8 mm with 2-mm interslice gaps to equal 10 mm, matrix 128×256, temporal resolution 40 ms or less, and field of view of 30–40 cm^2 depending on the patient's chest size. Breath-hold duration was 15–20 s per image sequence. To improve patient's comfort and compliance, data were acquired during the patient's end inspiration (moderate inspiration). The same acquisition was used to determine LV and RV parameters. Total data acquisition time was 20 min for cooperative patients with regular pacing and able to hold their breath.

Cardiac magnetic resonance calculations

Images were examined off-line using commercially available software (ARGUS, Siemens Medical Solutions). End-systole and end-diastole were not predefined, but contours were drawn on all phases and end-systole and end-diastole were automatically defined as the phases with the highest and lowest volumes.

CMR values were derived independently by the modified Simpson's rule from semiautomated regions that were modified manually to conform to endocardial borders [15,16]. Ventricular basal limits were defined as proposed by Alfakih *et al.* [25]. In line with the Society for Cardiovascular Magnetic Resonance recommendations, no corrections were carried out to compensate for papillary muscles, so as to simplify the CMR measurements for optimal reproducibility, saving post-processing time, and to use local institution normal reference ranges [24,26].

Gated blood-pool single-photon emission computed tomography data acquisition

Patients were injected with 740–925 MBq (20–25 mCi) of an in-vitro-labeled erythrocyte solution. Data were acquired using a dual-head γ-camera (Sopha DST-XL or Infinia Hawkeye 1; GE Healthcare, Chalfont St. Giles, UK) in a 90° configuration with low-energy high-resolution parallel-hole collimators. Tomographic gated blood-pool scintigraphy was performed with the following acquisition parameters: 5.6–6° per step (15–16 steps over 90° per head) for 180° according to American and European guidelines [27,28], 40-s acquisition per step, 10% R–R interval acceptance window, eight gated intervals, and 64×64 (pixel size: 5.9–6.8 mm). With these acquisition parameters, the examination time was 10–11 min for patients with regular pacing.

Gated blood-pool single-photon emission computed tomography processing

For all the patients in this study, 16 transverse slices were reconstructed for each time frame using filtered back-projection reconstruction. The projection data underwent compensation for scatter using the Jaszczak method [29]. Transverse slices were reoriented into the usual cardiac

axis and processed with inhouse semiautomatic GBPS software based on the watershed immersion algorithm (Tompool: freely available on the net at *http://www.scinti.etud.univ-montp1.fr*).

The GBPS algorithm described earlier [9,18,19,30] was modified and adapted to be run on standard desktop personal computers running under Windows operating systems (Microsoft Corp., Redmond, Washington, USA). Iterative thinnings that were used to produce a skeleton by influence zones [9] were replaced by a full three-dimensional immersion approach taking adjacent slices into consideration. This approach produced less over-segmentation of the ventricular cavities. To identify each segmented structure as belonging to the LV, the RV or the vascular structure behind the valve plane, septal, atrioventricular and pulmonary infundibulum planes were defined beforehand. Time–activity curves were generated using deformation of a reference curve as described by Caderas De Kerleau *et al.* [31]. These improvements led to a fully automatic algorithm, except for the precise location of the three aforementioned planes.

Statistics

Statistical analysis was carried out with commercially available software (SPSS for Windows, version 13.0; SPSS Inc., Chicago, Illinois, USA; and GraphPad Prism for Windows, version 5; GraphPad Software Inc., La Jolla, California, USA). The mean ± standard deviation characterizes the distributions of the parameters for the data. Continuous data were compared with a paired Student's *t*-test or a paired Wilcoxon test, as appropriate. Correlation among continuous variables was determined using linear regression and Spearman's rank order correlation coefficient (r_S). Bland–Altman analyses of measurement differences plotted versus mean values were used to assess biases (mean difference), trends, and 95% limits of agreement [32]. For all statistical testing, a two-tailed *P* value of less than 0.05 was considered statistically significant. The interoperator variability (*V*) of the semiautomatic tomographic method is expressed as the coefficient of variation of the paired measurements of EFs and volumes made by each of the two nuclear medicine physicians (D.M.-G. and L.S.) who used the program and analyzed the results of the segmentation procedure [33]:

$$V(\%) = 100 \times \frac{\sqrt{\sum_{i=1}^{n}(\mathrm{EF}_{1,i}-\mathrm{EF}_{2,i})^2}}{\mathrm{EF}_1 + \mathrm{EF}_2}$$

where $\mathrm{EF}_{1,i}$ and $\mathrm{EF}_{2,i}$ are the ith EFs (or volumes) measured by the first and second physicians, respectively, EF_1 and EF_2 are the mean EFs (or volumes) measured by the first and second physicians, respectively, and *n* is the number of measurements.

Results

GBPS was performed successfully in all patients and no complications occurred, whereas one patient was excluded from the CMR database on the basis of inadequate CMR gating (arrhythmia). The mean heart rate of the 29 remaining patients during the GBPS (66 ± 12 bpm) was not significantly different ($P = 0.31$) from that observed during the CMR (67 ± 12 bpm). All GBPS and CMR images were of sufficient image quality and suitable for analysis.

Algorithms were run for GBPS data for all 30 patients. Calculations of RVEF and LVEF and volumes using Tompool took less than 1 min per patient. CMR postprocessing was more time consuming: semimanual endocardial drawings required more than 30 min per patient (10 min for LV drawings and 20 min for RV drawings).

Using CMR as the reference, LV function was impaired in 13 (45%) patients and RV function was impaired in 5 (17%) patients.

Left ventricle

Main results are presented in Table 1.

Ejection fraction

LVEF assessed with GBPS and CMR were correlated [$r_s = 0.92$; $P < 0.001$; standard error of estimate (SEE) = 6.73%] (Fig. 1). Mean LVEF values for GBPS and CMR were not different (58 ± 19% and 56 ± 17%, respectively; $P = 0.063$). Figure 2 shows a Bland–Altman plot of LVEF measurements by GBPS and CMR. The results of the Bland–Altman analysis are summarized in Table 2, showing a mean difference of 2.4 and 95% limits of agreement of −10.7 to 15.5% for EF.

Volumes

LV EDV and ESV assessed with GBPS and CMR were correlated ($r_s = 0.82$; $P < 0.001$; SEE = 6.73 ml and $r_s = 0.82$; $P < 0.001$; SEE = 23.27 ml, respectively) (Fig. 3). The mean LV EDV and ESV values for GBPS and CMR were different (104 ± 57 ml; 140 ± 59 ml; $P < 0.001$ and 50 ± 51 ml; 69 ± 58 ml; $P < 0.001$, respectively). Figure 4 shows a Bland–Altman plot of LV EDV and ESV

Table 1 Left and right ventricular parameters assessed by GBPS and CMR ($n = 29$)

	Left ventricle		Right ventricle	
	GBPS	CMR	GBPS	CMR
EDV (ml)	104 ± 57*	140 ± 59*	92 ± 31*	103 ± 37*
ESV (ml)	50 ± 51*	69 ± 58*	45 ± 22	47 ± 25
SV (ml)	54 ± 18*	71 ± 19*	47 ± 15*	56 ± 21*
EF (%)	58 ± 19	56 ± 17	52 ± 10*	56 ± 11*

CMR, cardiac magnetic resonance; EDV, end-diastolic volume; EF, ejection fraction; ESV, end-systolic volume; GBPS, gated blood-pool single-photon emission computed tomography; SV, stroke volume.
*Significant differences in measurements ($P < 0.05$).

Fig. 1

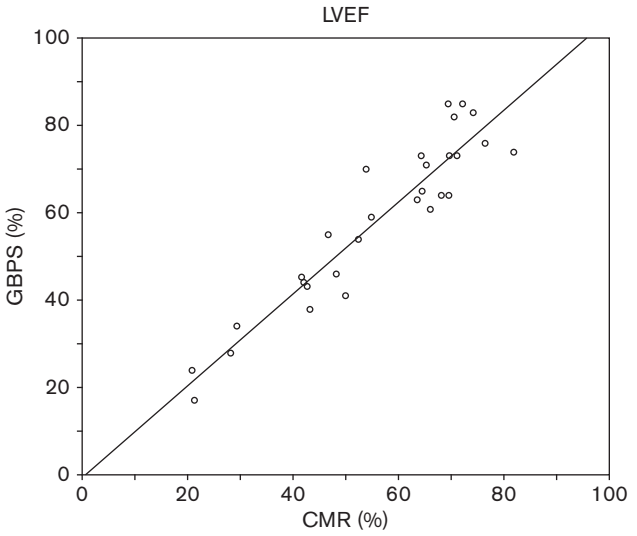

Correlation between gated blood-pool single-photon emission computed tomography (GBPS) and cardiac magnetic resonance (CMR) measurements of left ventricular (LV) ejection. $LVEF_{GBPS} = 1.05$ $LVEF_{CMR} - 0.55$; $R^2 = 0.88$; standard error of estimate $= 6.73$; $r_S = 0.92$; P less than 0.001.

Fig. 2

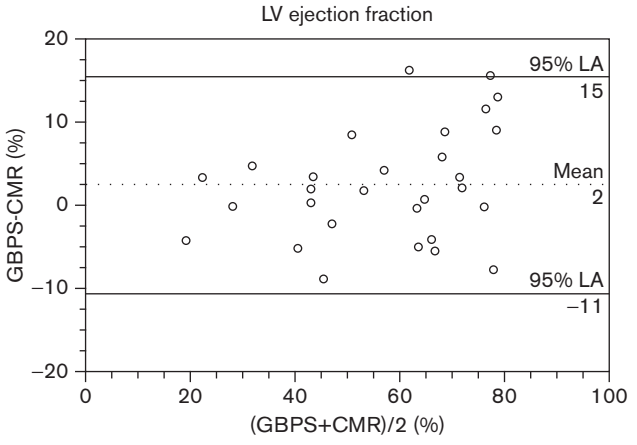

Left ventricular (LV) ejection fraction by Bland–Altman plotting. Horizontal lines indicate the mean difference and 95% limits of agreement (95% LA). CMR, cardiac magnetic resonance; GBPS, gated blood-pool single-photon emission computed tomography.

measurements by GBPS and CMR. The results of the Bland–Altman analysis showing for EDV a mean difference of −35.88 ml and 95% limits of agreement of −82.42 to 10.67 ml and for ESV a mean difference of −18.68 ml and 95% limits of agreements of −51.86 to 14.51 ml, are summarized in Table 3.

Right ventricle

The main results are presented in Table 1.

Table 2 Comparisons between GBPS and CMR measurements of left and right ventricular ejection fractions

	LVEF	RVEF
Correlation		
r_S	0.92	0.92
P	<0.001	<0.001
Regression line		
Slope	1.05	0.78
y_0	0.55	8.92
Difference (GBPS-CMR)		
Mean ± SD	2.40 ± 6.67	−3.63 ± 6.00
95% LA	(−10.68; 15.48)	(−15.39; 8.12)
SEM	1.24	1.11
95% CI	(−0.08; 4.88)	(−5.86; −1.40)
Bias	No	Yes

95% LA, 95% limits of agreement; CI, confidence interval; CMR, cardiac magnetic resonance; GBPS, gated blood-pool single-photon emission computed tomography; LVEF, left ventricular ejection fraction; RVEF, right ventricular ejection fraction; SD, standard deviation; SEM, standard error of the mean difference.

Fig. 3

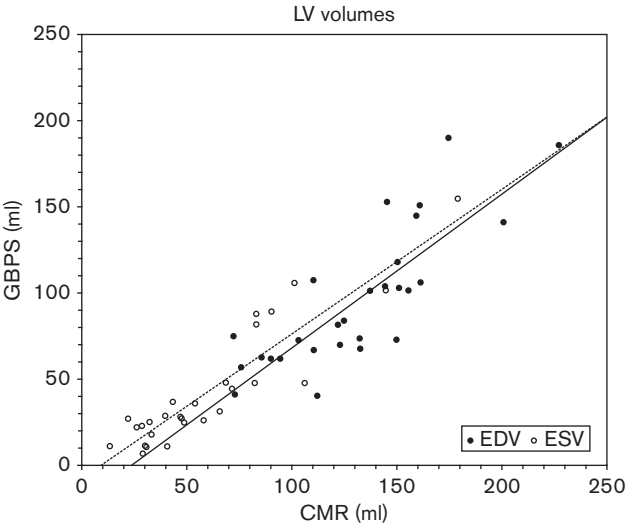

Correlation between gated blood-pool single-photon emission computed tomography (GBPS) and cardiac magnetic resonance (CMR) measurements of left ventricular (LV) end-diastolic volume (EDV) and end-systolic volume (ESV). $EDV_{GBPS} = 0.89$ $EDV_{CMR} - 20.61$; $R^2 = 0.84$; standard error of estimate $= 23.27$; $r_S = 0.82$; P less than 0.001. $ESV_{GBPS} = 0.84$ $ESV_{CMR} - 7.62$; $R^2 = 0.92$; standard error of estimate $= 14.37$; $r_S = 0.89$; P less than 0.001.

Ejection fraction

RVEF assessed with GBPS and CMR were correlated ($r_s = 0.74$; $P < 0.001$; SEE = 5.52%) (Fig. 5). The mean RVEF values for GBPS and CMR were different (52 ± 10% and 56 ± 11%, respectively; $P = 0.003$). Figure 6 shows a Bland–Altman plot of the RVEF measurements by GBPS and CMR. The results of the Bland–Altman analysis are summarized in Table 2, showing a mean difference of −3.63 and 95% limits of agreement of −15.39 to 8.12% for EF.

Volumes

RV EDV and ESV assessed with GBPS and CMR were correlated ($r_s = 0.80$; $P < 0.001$; SEE = 14.55 ml and $r_s = 0.86$; $P < 0.001$; SEE = 10.26 ml, respectively) (Fig. 7). The mean RV EDV values for GBPS and CMR were different (92 ± 31 ml and 103 ± 37 ml, respectively; $P = 0.001$). The mean RV ESV values for GBPS and CMR were not different (45 ± 22 ml and 47 ± 25 ml, respectively; $P_w = 0.136$). Figure 8 shows a Bland–Altman plot of RV EDV and ESV measurements by GBPS and CMR. The results of the Bland–Altman analysis are summarized in Table 3, showing a mean difference of −11.24 ml and 95% limits of agreement of −44.39 to 21.90 ml for EDV and a mean difference of −1.92 ml and 95% limits of agreement of −24.52 to 20.69 ml for ESV.

Stroke volumes

For the 24 patients without valvulopathy or shunt, LV stroke volume (SV) and RVSV were 54 ± 18 ml; 47 ± 15 ml for GBPS and 71 ± 19 ml; 56 ± 21 ml for CMR, respectively (Table 1). LVSV was significantly higher than RVSV with GBPS and CMR ($P = 0.003$ and $P < 0.001$, respectively). Means were significantly different between GBPS and CMR with, respectively, 9 ± 14 ml and 18 ± 13 ml ($P = 0.027$).

Interoperator variability

GBPS interoperator variability is, respectively, 0.6, 1.1%, and 1.7 for the LV EF, EDV, and ESV and 0.9, 1.8, and 2.5% for the RV EF, EDV, and ESV.

Fig. 4

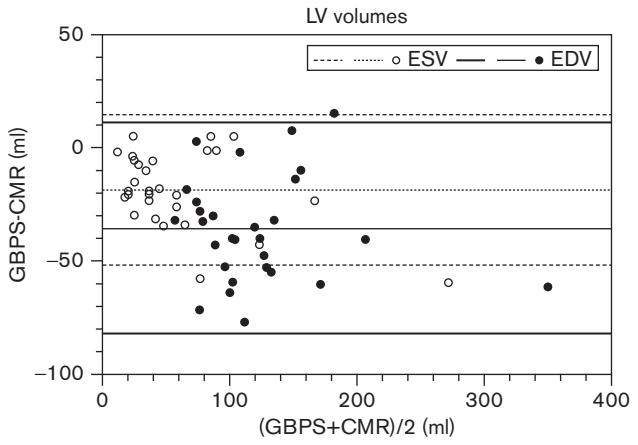

Left ventricular (LV) end-diastolic volume (EDV) and end-systolic volume (ESV) by Bland–Altman plotting. Horizontal lines indicate mean difference and 95% limits of agreement. CMR, cardiac magnetic resonance; GBPS, gated blood-pool single-photon emission computed tomography.

Fig. 5

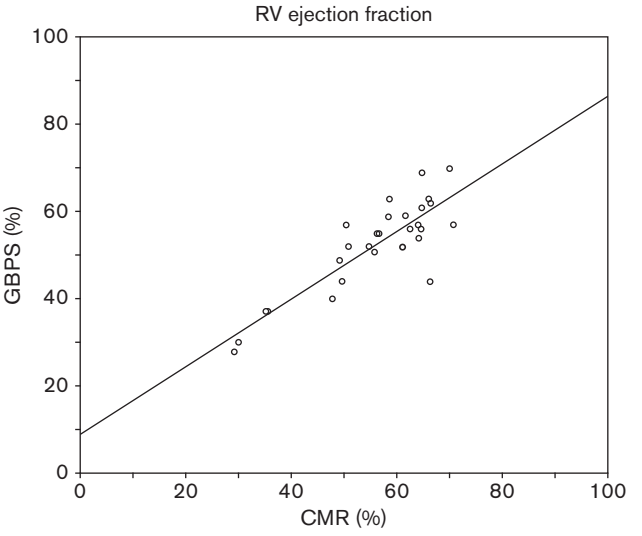

Correlation between gated blood-pool single-photon emission computed tomography (GBPS) and cardiac magnetic resonance (CMR) measurements of right ventricular (RV) ejection fraction (EF). $RVEF_{GBPS} = 0.78\ RVEF_{CMR} + 8.92$; $R^2 = 0.73$; standard error of estimate = 5.52; $r_S = 0.74$; P less than 0.001.

Table 3 Comparisons between GBPS and CMR measurements of left and right ventricular end-diastolic and end-systolic volumes

	LV EDV	LV ESV	RV EDV	RV ESV
Correlation				
r_S	0.84	0.89	0.80	0.86
P	<0.001	<0.001	<0.001	<0.001
Regression line				
Slope	0.89	0.84	0.75	0.78
y_0	−20.61	−7.62	14.01	8.44
Difference (GBPS-CMR)				
Mean ± SD	−35.88 ± 23.75	−18.68 ± 16.93	−11.24 ± 16.91	−1.92 ± 11.53
95% LA	(−82.42; 10.67)	(−51.86; 14.51)	(−44.39; 21.90)	(−24.52; 20.69)
SEM	4.41	3.14	3.14	2.14
95% CI	(−44.69; −27.06)	(−24.96; −12.39)	(−17.53; −4.96)	(−6.20; 2.37)
Bias	Yes	Yes	Yes	No

95% CI, 95% confidence interval; 95% LA, 95% limits of agreement; CMR, cardiac magnetic resonance; EDV, end-diastolic volume; ESV, end-systolic volume; GBPS, gated blood-pool single-photon emission computed tomography; LV, left ventricular; RV, right ventricular; SD, standard deviation; SEM, standard error of the mean difference.

Fig. 6

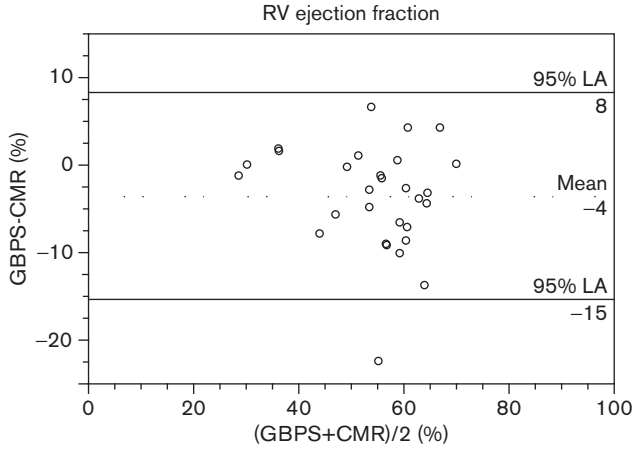

Right ventricular (RV) ejection fraction by Bland–Altman plotting. Horizontal lines indicate the mean difference and 95% limits of agreement (95% LA). CMR, cardiac magnetic resonance; GBPS, gated blood-pool single-photon emission computed tomography.

Fig. 7

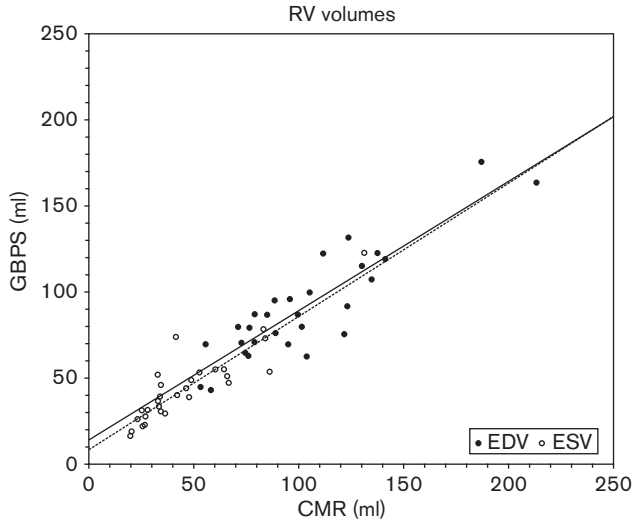

Correlation between gated blood-pool single-photon emission computed tomography (GBPS) and cardiac magnetic resonance (CMR) measurements of right ventricular (RV) end-diastolic volume (EDV) and end-systolic volume (ESV). $EDV_{GBPS} = 0.75$ $EDV_{CMR} + 14.01$; $R^2 = 0.79$; standard error of estimate = 14.55; $r_S = 0.80$; P less than 0.001. ESV_{GBPS} 0.78 $EDV_{CMR} + 8.44$; $R^2 = 0.79$; standard error of estimate = 10.26; $r_S = 0.86$; P less than 0.001.

Fig. 8

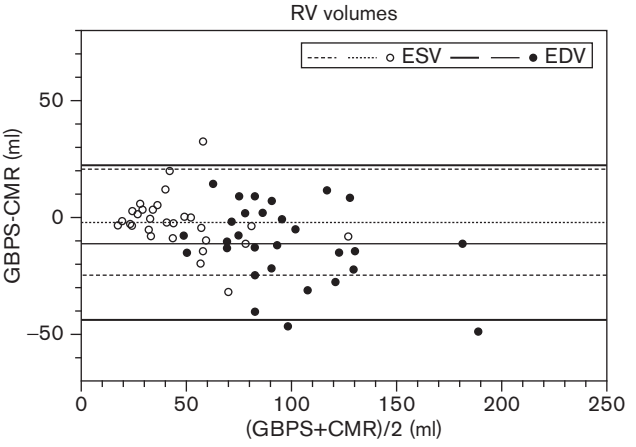

Right ventricular (RV) end-diastolic volume (EDV) and end-systolic volume (ESV) by Bland–Altman plotting. Horizontal lines indicate mean difference and 95% limits of agreement (95% LA). CMR, cardiac magnetic resonance; GBPS, gated blood-pool single-photon emission computed tomography.

Discussion

A few studies have compared GBPS with CMR measurements using current steady-state-free precession sequences [21,34–36]. Our investigation shows that both LV and RV functions can be simultaneously, easily, and rapidly obtained using GBPS with a count-based method whose results are in close agreement with those provided by CMR. Correlations were found between GBPS and CMR for all parameters. Using only eight-frame GBPS, we did not find systematic underestimation of EF, thus confirming the results from earlier studies [31,37]. The wider limits of agreement between GBPS and CMR for RVEF can be partly explained by the increased variability in the postprocessing data for the RV using CMR [13] and GBPS [9,18]. With regard to CMR, this was mainly because of the difficulty of defining the most basal slice in the short-axis view and the upper limit of the RV between the ventricle and the pulmonary artery. With regard to GBPS, the pulmonary valve plane was chosen by detecting the changes in shape at the superior border of the RV at end-diastole. This inevitably introduced uncertainty but seemed to be more appropriate for patients with cardiac dilatation than the method used by Chin *et al.* [38] who defined the upper border of the RV as the transverse slice above the superior border of the LV at end-diastole. However, the clinical impact of such low variability has not been shown.

Despite their totally different approaches (count-based for GBPS and based on modified Simpson's rule for CMR), the volume measurements were in quite close agreement. However, bias, trends, and wider limits of agreement were found for the highest LV and RV volumes. Several factors may explain this finding. One is the self-attenuation by the blood pools of radiation emanating from ventricles. This assumption may be correct especially in patients with dilated cardiomyopathy. As large volumes are more influenced than smaller volumes by radiation attenuation, this might partially explain the increasing volume differences between GBPS and CMR. Volumes obtained by GBPS are probably

slightly underestimated because of radiation attenuation; further study using computed tomography based attenuation correction is necessary. Another factor is the inclusion of papillary muscles and trabeculations in performing CMR cavity drawings. Trabeculae significantly affect quantifications of LV volume [39]. Higher mean percentage differences between CMR and GBPS in ESV measurements than in EDV are in support of this hypothesis. Lastly, the use of the short axis in performing CMR measurements leads to the problem of determining atrioventricular planes on most basal slices. This generates more variability than the horizontal long-axis method for the RV [40] or the radial long-axis method for the LV [41].

Twenty-four patients without any significant valvulopathy or ventricular communication were included in the further analysis of SV. For these patients, it was clear that no difference between LVSV and RVSV should exist. Using CMR and GBPS independently to assess LVSV and RVSV, we found a significant difference for both techniques, with higher LVSV than RVSV. This confirmed the earlier published results comparing GBPS and thermodilution measurements [18]. The mean differences between SV were two times smaller using GBPS than CMR. However, Alfakih *et al.* [40] found a smaller difference of 7.4 ± 10.8 ml between LVSV and RVSV using CMR with the exclusion of two papillary muscles from the LV cavity (18 ± 13 ml in our study). This result is in close agreement with our GBPS finding, thus indicating that a similar degree of accuracy in volume measurements can be obtained, with a more sophisticated and therefore less reproducible analysis of MRI studies.

CMR is often used for quantifying LVEF or RVEF and volumes. This CMR, which does not use ionizing radiation, has one major advantage over scintigraphic techniques. Nevertheless, CMR is not widely available and has limited feasibility in patients with implanted devices or claustrophobia. It also requires considerable expertize and involves time-consuming data processing (more than 30 min for both ventricles) because of the lack of a commercially available segmentation method. Cost should also be considered in the overall evaluation of the technique [42]. Manual or semiautomatic processing of CMR data also leads to decreased reproducibility, with a mean interobserver difference of $-2.5 \pm 2.5\%$ for LVEF and $2.9 \pm 5.8\%$ for RVEF in healthy individuals [43]. Our study shows close correlation and agreement between EF and volumes assessed by GBPS and CMR. The results could be improved by modifications to both techniques, and they need to be validated further in a larger number of patients with a greater frequency of severe dysfunction.

Conclusion

EF and volume measurements by GBPS showed correlation and close agreement with CMR calculations, with no requirement for a highly qualified physician and rapid procedures for data analysis. This suggests that this simple and widely available technique is a clinically useful tool for assessing both LV and RV functions.

Acknowledgement

There is no conflict of interest to declare.

References

1 White HD, Norris RM, Brown MA, Brandt PW, Whitlock RM, Wild CJ. Left ventricular end-systolic volume as the major determinant of survival after recovery from myocardial infarction. *Circulation* 1987; **76**:44–51.
2 Sharir T, Germano G, Kavanagh PB, Lai S, Cohen I, Lewin HC, *et al.* Incremental prognostic value of post-stress left ventricular ejection fraction and volume by gated myocardial perfusion single photon emission computed tomography. *Circulation* 1999; **100**:1035–1042.
3 Wang TJ, Evans JC, Benjamin EJ, Levy D, LeRoy EC, Vasan RS. Natural history of asymptomatic left ventricular systolic dysfunction in the community. *Circulation* 2003; **108**:977–982.
4 Ghio S, Gavazzi A, Campana C, Inserra C, Klersy C, Sebastiani R, *et al.* Independent and additive prognostic value of right ventricular systolic function and pulmonary artery pressure in patients with chronic heart failure. *J Am Coll Cardiol* 2001; **37**:183–188.
5 Lee DS, Ahn JY, Kim SK, Oh BH, Seo JD, Chung JK, *et al.* Limited performance of quantitative assessment of myocardial function by thallium-201 gated myocardial single-photon emission tomography. *Eur J Nucl Med* 2000; **27**:185–191.
6 Manrique A, Faraggi M, Vera P, Vilain D, Lebtahi R, Cribier A, *et al.* ^{201}Tl and ^{99m}Tc-MIBI gated SPECT in patients with large perfusion defects and left ventricular dysfunction: comparison with equilibrium radionuclide angiography. *J Nucl Med* 1999; **40**:805–809.
7 Vallejo E, Dione DP, Bruni WL, Constable RT, Borek PP, Soares JP, *et al.* Reproducibility and accuracy of gated SPECT for determination of left ventricular volumes and ejection fraction: experimental validation using MRI. *J Nucl Med* 2000; **41**:874–882. discussion 83–86.
8 Nichols K, DePuey EG, Krasnow N, Lefkowitz D, Rozanski A. Reliability of enhanced gated SPECT in assessing wall motion of severely hypoperfused myocardium: echocardiographic validation. *J Nucl Cardiol* 1998; **5**:387–394.
9 Mariano-Goulart D, Collet H, Kotzki PO, Zanca M, Rossi M. Semi-automatic segmentation of gated blood pool emission tomographic images by watersheds: application to the determination of right and left ejection fractions. *Eur J Nucl Med* 1998; **25**:1300–1307.
10 Gandy SJ, Waugh SA, Nicholas RS, Simpson HJ, Milne W, Houston JG. Comparison of the reproducibility of quantitative cardiac left ventricular assessments in healthy volunteers using different MRI scanners: a multicenter simulation. *J Magn Reson Imaging* 2008; **28**:359–365.
11 Gandy SJ, Waugh SA, Nicholas RS, Rajendra N, Martin P, Houston JG. MRI comparison of quantitative left ventricular structure, function and measurement reproducibility in patient cohorts with a range of clinically distinct cardiac conditions. *Int J Cardiovasc Imaging* 2008; **24**:627–632.
12 Koskenvuo JW, Karra H, Lehtinen J, Niemi P, Parkka J, Knuuti J, *et al.* Cardiac MRI: accuracy of simultaneous measurement of left and right ventricular parameters using three different sequences. *Clin Physiol Funct Imaging* 2007; **27**:385–393.
13 Grothues F, Moon JC, Bellenger NG, Smith GS, Klein HU, Pennell DJ. Interstudy reproducibility of right ventricular volumes, function, and mass with cardiovascular magnetic resonance. *Am Heart J* 2004; **147**:218–223.
14 Barkhausen J, Ruehm SG, Goyen M, Buck T, Laub G, Debatin JF. MR evaluation of ventricular function: true fast imaging with steady-state precession versus fast low-angle shot cine MR imaging: feasibility study. *Radiology* 2001; **219**:264–269.
15 Thiele H, Paetsch I, Schnackenburg B, Bornstedt A, Grebe O, Wellnhofer E, *et al.* Improved accuracy of quantitative assessment of left ventricular volume and ejection fraction by geometric models with steady-state free precession. *J Cardiovasc Magn Reson* 2002; **4**:327–339.
16 Dulce MC, Mostbeck GH, Friese KK, Caputo GR, Higgins CB. Quantification of the left ventricular volumes and function with cine MR imaging: comparison of geometric models with three-dimensional data. *Radiology* 1993; **188**:371–376.
17 Daou D, Harel F, Helal BO, Fourme T, Colin P, Lebtahi R, *et al.* Electrocardiographically gated blood-pool SPECT and left ventricular

function: comparative value of 3 methods for ejection fraction and volume estimation. *J Nucl Med* 2001; **42**:1043–1049.
18 Mariano-Goulart D, Piot C, Boudousq V, Raczka F, Comte F, Eberle MC, *et al.* Routine measurements of left and right ventricular output by gated blood pool emission tomography in comparison with thermodilution measurements: a preliminary study. *Eur J Nucl Med* 2001; **28**:506–513.
19 Mariano-Goulart D, Dechaux L, Rouzet F, Barbotte E, Caderas de Kerleau C, Rossi M, *et al.* Diagnosis of diffuse and localized arrhythmogenic right ventricular dysplasia by gated blood-pool SPECT. *J Nucl Med* 2007; **48**:1416–1423.
20 Caderas de Kerleau C, Ahronovitz E, Rossi M, Mariano-Goulart D. Automatic ventricular wall motion analysis by gated blood-pool emission tomography using deformations of an ideal time–activity curve. *IEEE Trans Med Imaging* 2004; **23**:485–491.
21 Nichols KJ, Van Tosh A, Wang Y, Palestro CJ, Reichek N. Validation of gated blood-pool SPECT regional left ventricular function measurements. *J Nucl Med* 2009; **50**:53–60.
22 Nichols KJ, Van Tosh A, De Bondt P, Bergmann SR, Palestro CJ, Reichek N. Normal limits of gated blood pool SPECT count-based regional cardiac function parameters. *Int J Cardiovasc Imaging* 2008; **24**:717–725.
23 Carr JC, Simonetti O, Bundy J, Li D, Pereles S, Finn JP. Cine MR angiography of the heart with segmented true fast imaging with steady-state precession. *Radiology* 2001; **219**:828–834.
24 Kramer CM, Barkhausen J, Flamm SD, Kim RJ, Nagel E. Standardized cardiovascular magnetic resonance imaging (CMR) protocols, society for cardiovascular magnetic resonance: board of trustees task force on standardized protocols. *J Cardiovasc Magn Reson* 2008; **10**:35.
25 Alfakih K, Reid S, Jones T, Sivananthan M. Assessment of ventricular function and mass by cardiac magnetic resonance imaging. *Eur Radiol* 2004; **14**:1813–1822.
26 Sievers B, Kirchberg S, Bakan A, Franken U, Trappe HJ. Impact of papillary muscles in ventricular volume and ejection fraction assessment by cardiovascular magnetic resonance. *J Cardiovasc Magn Reson* 2004; **6**:9–16.
27 Hansen CL, Goldstein RA, Akinboboye OO, Berman DS, Botvinick EH, Churchwell KB, *et al.* Myocardial perfusion and function: single photon emission computed tomography. *J Nucl Cardiol* 2007; **14**:e39–e60.
28 Hesse B, Lindhardt TB, Acampa W, Anagnostopoulos C, Ballinger J, Bax JJ, *et al.* EANM/ESC guidelines for radionuclide imaging of cardiac function. *Eur J Nucl Med Mol Imaging* 2008; **35**:851–885.
29 Jaszczak RJ, Floyd CE, Coleman RE. Scatter compensation techniques for SPECT. *IEEE Trans Nucl Sci* 1985; **32**:786–793.
30 Mariano-Goulart D, Caderas de Kerleau C, Rossi M. Automatic measurements of local ventricular parameters using Gated Blood-Pool Emission tomography. *Méd Nucl* 2005; **29**:115–130.
31 Caderas de Kerleau C, Crouzet JF, Ahronovitz E, Rossi M, Mariano-Goulart D. Automatic generation of noise-free time-activity curve with gated blood-pool emission tomography using deformation of a reference curve. *IEEE Trans Med Imaging* 2004; **23**:485–491.
32 Bland JM, Altman DG. Statistical methods for assessing agreement between two methods of clinical measurement. *Lancet* 1986; **1**:307–310.
33 Nilas L, Hassager C, Christiansen C. Long-term precision of dual photon absorptiometry in the lumbar spine in clinical settings. *Bone Miner* 1988; **3**:305–315.
34 Akinboboye O, Nichols K, Wang Y, Dim UR, Reichek N. Accuracy of radionuclide ventriculography assessed by magnetic resonance imaging in patients with abnormal left ventricles. *J Nucl Cardiol* 2005; **12**:418–427.
35 Kjaer A, Lebech AM, Hesse B, Petersen CL. Right-sided cardiac function in healthy volunteers measured by first-pass radionuclide ventriculography and gated blood-pool SPECT: comparison with cine MRI. *Clin Physiol Funct Imaging* 2005; **25**:344–349.
36 Harel F, Finnerty V, Gregoire J, Thibault B, Marcotte F, Ugolini P, *et al.* Gated blood-pool SPECT versus cardiac magnetic resonance imaging for the assessment of left ventricular volumes and ejection fraction. *J Nucl Cardiol* 2010; **17**:427–434.
37 Kim SJ, Kim IJ, Kim YS, Kim YK. Gated blood pool SPECT for measurement of left ventricular volumes and left ventricular ejection fraction: comparison of 8 and 16 frame gated blood pool SPECT. *Int J Cardiovasc Imaging* 2005; **21**:261–266.
38 Chin BB, Bloomgarden DC, Xia W, Kim HJ, Fayad ZA, Ferrari VA, *et al.* Right and left ventricular volume and ejection fraction by tomographic gated blood-pool scintigraphy. *J Nucl Med.* 1997; **38**:942–948.
39 Papavassiliu T, Kuhl HP, Schroder M, Suselbeck T, Bondarenko O, Bohm CK, *et al.* Effect of endocardial trabeculae on left ventricular measurements and measurement reproducibility at cardiovascular MR imaging. *Radiology* 2005; **236**:57–64.
40 Alfakih K, Plein S, Bloomer T, Jones T, Ridgway J, Sivananthan M. Comparison of right ventricular volume measurements between axial and short axis orientation using steady-state free precession magnetic resonance imaging. *J Magn Reson Imaging* 2003; **18**:25–32.
41 Bloomer TN, Plein S, Radjenovic A, Higgins DM, Jones TR, Ridgway JP, *et al.* Cine MRI using steady state free precession in the radial long axis orientation is a fast accurate method for obtaining volumetric data of the left ventricle. *J Magn Reson Imaging* 2001; **14**:685–692.
42 Pennell DJ, Sechtem UP, Higgins CB, Manning WJ, Pohost GM, Rademakers FE, *et al.* Clinical indications for cardiovascular magnetic resonance (CMR): consensus panel report. *J Cardiovasc Magn Reson* 2004; **6**:727–765.
43 Alfakih K, Plein S, Thiele H, Jones T, Ridgway JP, Sivananthan MU. Normal human left and right ventricular dimensions for MRI as assessed by turbo gradient echo and steady-state free precession imaging sequences. *J Magn Reson Imaging* 2003; **17**:323–329.